ACS APPLIED MATERIALS & INTERFACES

Research Article

www.acsami.org

Fabrication of Thorny Au Nanostructures on Polyaniline Surfaces for Sensitive Surface-Enhanced Raman Spectroscopy

Siwei Li,[†] Ping Xu,*[,†,‡] Ziqiu Ren,[†] Bin Zhang,[†] Yunchen Du,[†] Xijiang Han,[†] Nathan H. Mack,[‡] and Hsing-Lin Wang*[,‡]

[†]Department of Chemistry, Harbin Institute of Technology, Harbin 150001, China

[‡]Chemistry Division, Los Alamos National Laboratory, Los Alamos, New Mexico 87545, United States

Supporting Information

ABSTRACT: Here we demonstrate, for the first time, the fabrication of Au nanostructures on polyaniline (PANI) membrane surfaces for surface enhanced Raman spectroscopy (SERS) applications, through a direct chemical reduction by PANI. Introduction of acids into the $HAuCl_4$ solution leads to homogeneous Au structures on the PANI surfaces, which show only sub-ppm detection levels toward the target analyte, 4-mercaptobenzoic acid (4-MBA), because of limited surface area and lack of surface roughness. Thorny Au nanostructures can be obtained through controlled reaction conditions and the addition of a capping agent poly (vinyl pyrrolidone) (PVP) in the $HAuCl_4$ solution and the temperature kept at 80 °C in an oven. Those thorny Au nanostructures, with higher surface areas and unique geometric feature, show a SERS detection sensitivity of 1×10^{-9} M (sub-ppb level) toward two different analyte molecules, 4-MBA and Rhodamine B, demonstrating their generality for SERS applications. These highly sensitive SERS-active substrates offer novel robust structures for trace detection of chemical and biological analytes.

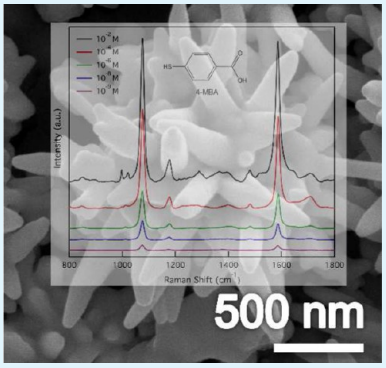

KEYWORDS: *surface enhanced Raman spectroscopy, gold, polyaniline, thorny nanostructures*

1. INTRODUCTION

Surface-enhanced Raman spectroscopy (SERS) mainly utilizes the greatly enhanced electromagnetic field as well as the localized surface plasmon resonances generated at the metal surfaces to get enhanced Raman signal of a target molecule.[1−3] SERS has been recognized as a potentially powerful technique for trace detection of chemical and biological molecules at the single molecule level.[4−7] Since its first discovery on roughened metal electrodes,[8−10] pursuit of highly sensitive and active SERS substrates has never been stopped. Up to now, various designs of SERS-active substrates have been reported, including roughened metal substrates,[11−14] metal nanoparticle assemblies,[15−21] porous or holey substrates,[22−24] and even semiconductor-based substrates.[25−28] Despite these successful fabrication-based approaches in making highly uniform substrates, there remains a need for SERS-active materials that are highly sensitive, reproducible, cost-effective, and a platform enables multiple substrate designs (i.e., flexible).

To overcome some of the hurdles associated with traditionally fabricated SERS substrates, we have taken advantage of the redox chemistry of conjugated polymers to spontaneously reduce metal ions with appropriate reduction potentials to zerovalent metals. It has been demonstrated that conjugated polymers like polyaniline (PANI), polypyrrole (PPy), and PANI-PPy copolymers can be used as reducing agents to synthesize noble metal nanoparticles.[29−36] Especially, when we process the PANI powders into PANI membranes or films, metals like Ag, Au, Pt, and Pd can be spontaneously grown on the PANI surfaces through the direct chemical deposition technique, where the size and morphology of the metal structures can be manipulated by the chemical nature and surface chemistry of PANI, and reaction conditions like temperature, metal salt concentration, reaction time, etc.[29−36] The Pt and Pd nanoparticles on PANI surfaces are found to be highly efficient heterogeneous catalysts toward specific reactions in organic synthesis.[37,38] Moreover, we have demonstrated that Ag nanostructures fabricated on the PANI surface can be highly sensitive SERS platforms in detection of chemical molecules, with a detection sensitivity as high as 1×10^{-12} M.[31−36] However, all attempts to produce Au nanostructures with high SERS activities have been limited, as Au growth on PANI surface typically results in featureless Au with few SERS-favorable morphologies.[32]

In this paper, we demonstrate the first example of Au nanostructures grown on PANI membranes using elevated temperature (80 °C) and a capping agent poly (vinyl pyrrolidone) (PVP) to yield thorny Au nanostructures with high aspect ratio and radius of curvature. These Au nanostructures show high SERS sensitivity (up to sub-ppb level) toward a model analyte, 4-mercaptobenzoic acid (4-

Received: September 4, 2012
Accepted: December 12, 2012
Published: December 12, 2012

   dx.doi.org/10.1021/am301881q | ACS Appl. Mater. Interfaces 2013, 5, 49−54

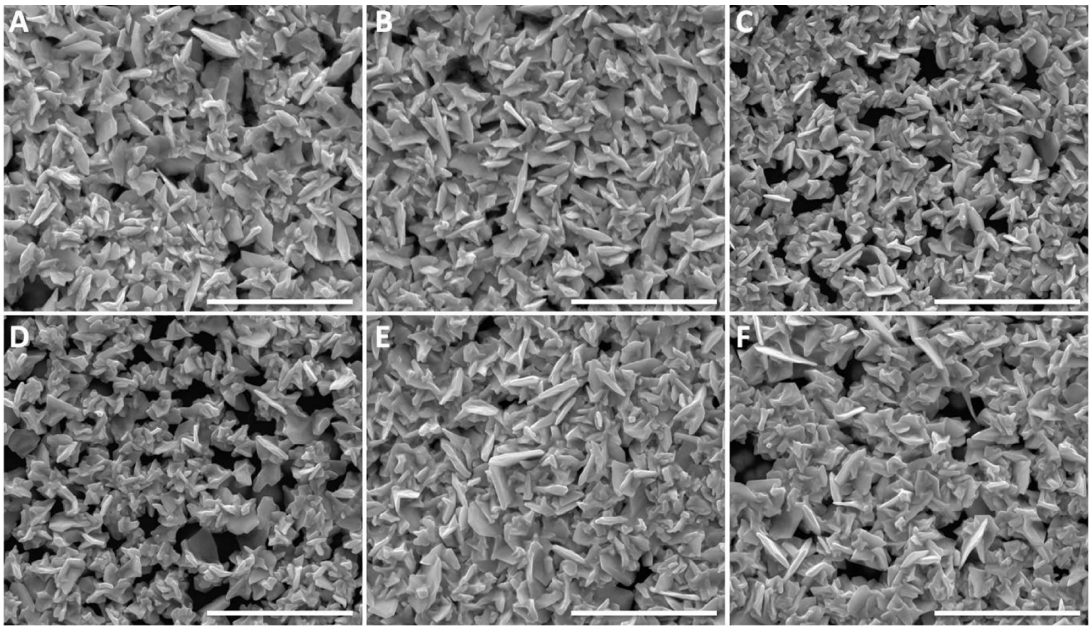

Figure 1. SEM images of the Au nanostructures obtained by immersing undoped PANI membranes (5 mm × 5 mm pieces) in a mixture solution of 1 mL of 25 mM $HAuCl_4$ and (A) 50 μL of 0.25 M citric acid, (B) HNO_3, (C) mandelic acid, (D) camphorsulfonic acid, (E) HBF_4, and (F) toluenesulfonic acid for 30 min. The reactions were carried out at room temperature. Scale bar: 3 μm.

MBA). We believe the as-prepared Au nanostructures are a promising material for the real time detection of chemical and biological molecule.

2. EXPERIMENTAL SECTION

Materials. PANI emeraldine base (EB) powder (average MW: ~50 000, Aldrich), *N*-Methyl-2-pyrrolidone (NMP, 99% Aldrich), heptamethylenimine (HPMI, 98% Acros), poly (Vinyl Pyrrolidone) (PVP, Aldrich, M.W. = 40 000), gold(III) chloride hydrate (HAuCl4 99.999% Aldrich), *R*-(-)-camphorsulfonic acid (98% Aldrich), *R*-(-)-mandelic acid (99% Aldrich), citric acid (99.9% Fisher), *p*-toluenesulfonic acid (>98% Aldrich),HBF_4 (48 wt %, Aldrich), HNO_3 (70%, Aldrich), and 4-mercaptobenzoic acid (4-MBA, Aldrich 90%) were used as received.

Fabrication of PANI Membranes. PANI membranes are fabricated by a phase inversion method using water as the coagulation bath.[32] In a typical experiment, 1.15 g of PANI (EB) powder, 4.14 g of NMP, and 0.747 g of HPMI were mixed in a 12 mL of Teflon vial. The mixture was stirred for 0.5−1 h to form a homogeneous solution, followed by being poured onto a glass substrate and spread into a wet film using a gardener's blade with a controlled thickness. The wet film was then immersed into a water bath and kept in the water bath for at least 24 h. The resulting membrane was then dried at room temperature for 6 h, and then cut into 5 mm × 5 mm pieces. A part of the PANI pieces was doped in 0.25 M citric acid for 3 days before being used for Au growth, and others remain undoped.

Growth of Au Nanostructures on PANI Membranes. The growth of Au nanostructures on PANI surface was conducted as follows: one piece of undoped or doped PANI membrane was immersed in the reaction system for a period of time. Here, two different reaction systems are applied to study the Au growth on PANI surfaces: (1) the reaction solution contains 1 mL 25 mM $HAuCl_4$ and 50 μL 0.25 M acid solution (citric acid, HNO_3, mandelic acid, camphorsulfonic acid, HBF_4 or toluenesulfonic acid), and the reaction was carried out at room temperature; (2) the reaction system is a mixture solution of 0.1 M PVP and 5 mM $HAuCl_4$, and the reaction was carried out in an oven kept at 80 °C. After Au growth, the PANI membranes were washed by water at least 5 times in order to remove the surface-adsorbed PVP molecules as much as possible, and then dried in air.

Characterization. Scanning electron microscopic (SEM) images were taken on a FEI Inspect SEM. The characteristics of the crystallite structure of the prepared samples were determined using an XRD-6000 X-ray diffractometer (Shimadzu) with a Cu Kα radiation source (λ = 1.5405 Å, 40.0 kV, and 30.0 mA). For SERS measurement, the PANI membranes after Au growth were immersed in 4-MBA ethanol solutions and Rhodamine B aqueous solutions of different concentrations for 30 min, and then washed with ethanol thoroughly. The Raman spectra were recorded on a Renishaw in Via micro Raman spectroscopy system, using the TE air-cooled 576 × 400 CCD array in a confocal Raman system (wavelength: 633 nm). The incident laser power was kept at 5 mW and total accumulation times of 2 s were employed.

3. RESULTS AND DISCUSSION

The freestanding PANI membranes are then directly immersed into a $HAuCl_4$ solution for a controlled time period to spontaneously reduce the metal ions into metal nanostructures. As can be seen from our previous works,[29,32] immersing the PANI membranes directly into the $HAuCl_4$ solution for less than 1 min only leads to Au nanoparticles or their assemblies. Even after a longer reaction time, one can only see scattered Au particles on the PANI surface (see Figure S1 in the Supporting Information). And we can get very limited SERS signals from these Au nanoparticles. As SERS "hot spots" usually reside in the interstitial voids of metal nanoparticles and metal structures with intersections, bifurcations, and high radius of curvatures,[1,32] exquisite preparation of metal nanoparticles with controlled size and morphology and delicate manipulation of the nanoparticle assemblies are required in order to maximize the sensitivity of the prepared SERS platforms. Therefore, to truly realize efficient SERS-active Au materials, control over the morphology or assembly of Au nanostructures on PANI is required.

Our previous studies on Ag growth on PANI show that introduction of specific organic acids into the $AgNO_3$ solution results in homogeneous Ag nanostructures even on undoped PANI membranes and the morphology of the Ag nanostruc-

tures can be well tuned by the chemical nature of the organic acid.[36] In this work, we attempt to apply similar procedures to affect the growth of Au nanostructures. As can be seen from Figure 1, the introduction of citric acid, HNO_3, mandelic acid, camphorsulfonic acid, HBF_4 and toluenesulfonic acid in the $HAuCl_4$ solution all results in similarly homogeneous Au nanostructures on the PANI surface. These Au structures are actually composed of assembled sheet-like units, with each acid contributing to only slight differences in size and thickness. These structural similarities are presumably the result of two congruent processes occurring at the time of metal deposition: (1) as we previously discovered,[36] in situ doping of PANI surface by the acid molecules can create a homogeneous distribution of active nucleation sites for Au^{3+} ions, so we can get homogeneous Au structures on PANI surfaces; and (2) the acid molecules adsorbed on Au nuclei surfaces will not change the nucleation and growth of Au crystals that much as on Ag surfaces, presumably because of the more inert nature of the Au crystal planes. Therefore, very similar Au nanostructures are produced regardless of the chemical nature of the acids.

To study the SERS responses of the as-prepared Au nanostructures, we selected 4-mercaptobenzoic acid (4-MBA) as the target molecule here. 4-MBA, an organic molecule with a thiol group on one end and a carboxylic acid on the other end, usually has strong chemical interactions with metal surfaces. The Raman spectrum of 4-MBA is dominated by the ν_{8a} (~1590 cm^{-1}) and ν_{12} (~1080 cm^{-1}) aromatic ring vibrations; other weak bands at ~1150 and ~1180 cm^{-1} are attributed to the C−H deformation modes.[39] The similar Au nanostructures that are produced from the different acids introduced during metal growth are expected to yield similar SERS responses; For clarity, this work focuses on the sample prepared with the assistance of citric acid (see Figure 1A). It is somehow disappointing that the detection limit of 4-MBA on the homogeneous Au nanostructures can only reach 1×10^{-6} M, which is at a subppm level, and one can barely see any signals at a concentration of 1×10^{-7} M (Figure 2). Au nanostructures prepared from other acids show similar trends in their SERS sensitivities. It is important to note that, these concentration studies represent an ideal detection scenario, where the model analyte readily adsorbs to the metal surface through the S−Au covalent bond. It is expected that the metal surface is covered by a monolayer of 4-MBA molecules whose surface coverage is dominated by the concentration. However, the SEM images in Figure 1 indicate a relatively low surface area for all of the Au structures; thus the molecules adsorbed on the Au surfaces will be very limited. Meanwhile, the enhancement of electromagnetic field at the Au surfaces might be also very limited because of the lack of features (e.g., nanoscale roughness) that would create enough SERS "hot spots". Therefore, only a subparts per million level sensitivity can be obtained from these Au structures.

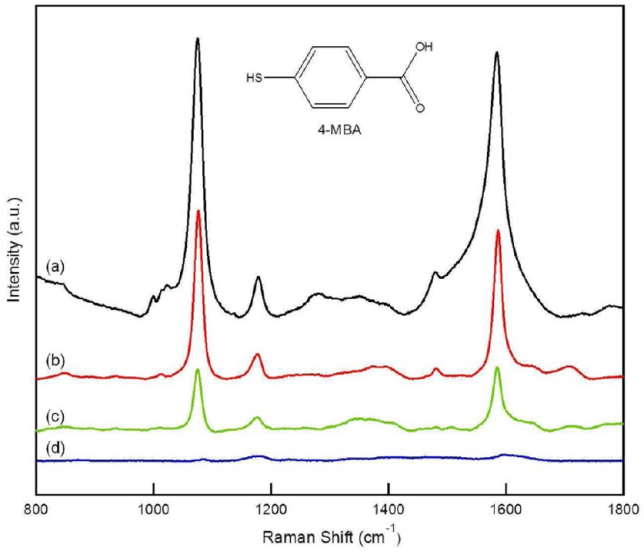

Figure 2. Concentration-dependent SERS spectra of 4-MBA on the Au nanostructures prepared by immersing the undoped PANI membrane in a mixture solution of citric acid and $HAuCl_4$ for 30 min: (a) 1×10^{-2} M, (b) 1×10^{-4} M, (c) 1×0^{-6} M, (d) 1×10^{-7} M.

Since the introduction of acid into the reaction system failed to bring the versatility of Au nanostructures as we got for Ag nanostructures and in an effort to enhance these sensitivity levels, we tried the Au growth at a higher temperature (80 °C), which results in readily apparent increases in Au growth rates. Immersing an undoped PANI membrane in a 5 mM $HAuCl_4$ solution kept at 80 °C in an oven immediately produces a shiny Au film on the PANI surface. However, it turns out that the shiny Au layer is actually composed of large bulk Au crystals, with microsized features (see Figure S2 in the Supporting Information). To arrest this fast Au growth, a widely studied capping agent, poly (vinyl pyrrolidone) (PVP), was introduced into the reaction system. PVP is known to affect the growth rate of certain metal crystal planes, and may enable some degree of morphology control during the spontaneous metal reduction process.[40−42] Here, Au growth in a reaction system of 0.1 M PVP and 5 mM$HAuCl_4$ at 80 °C was found to have dramatically slower growth rates. Figure 3 shows the SEM images of the Au nanostructures as a function of increasing exposure time to the growth solution, which are very different from those grown on PANI surfaces by introducing acids in the reaction solution (See Figure 1). At 5 min, one can see particles that are 1−2 μm in size from the low magnification image (Figure 3A). Upon close examination (Figure 3B), needlelike nanostructures with diameters of about 30−50 nm are found to grow out of the Au crystals. Interestingly, these needlelike structures grow in size nad become better defined with prolonged reaction periods, and thorny structures are produced on the PANI surfaces (Figure 3C, E). From the magnified SEM images (Figure 3D, F), one can find that the growth seems to emanate from a common nucleation point with numerous nanoneedles sharing the same central core, and the diameter of the nanoneedles becomes larger with a longer reaction period, which is about 50−80 nm at 15 min, and 100−120 nm at 30 min. However, when we further increase the reaction time to 60 min, the needles begin to coalesce into large Au sheets (Figures 3G,H), which are similar in structure to the low-temperature, acid-assisted structures. Presumably, this process follows an Ostwald ripening route where the ripening effect has been significantly slowed by the PVP such that it occurs over the course of an hour. The acid only and high temperature synthesis conditions do not produce any needle-like features because the ripening occurs immediately and therefore the initial fine Au structures are hided. A similar increase in the ripening of the Au structures is observed when higher concentrations of $HAuCl_4$ solution are used. For example, when a 15 mM $HAuCl_4$ solution is used, featureless Au particles with sizes of 1−2 μm are produced in less than 5 min (see Figure S3 in the Supporting Information).

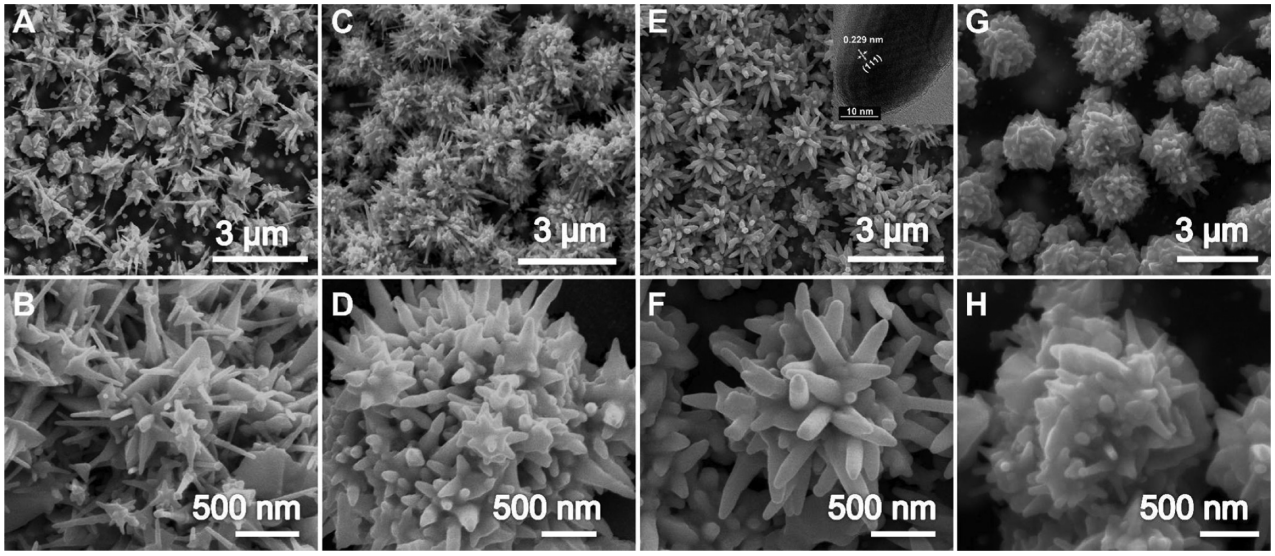

Figure 3. SEM images of Au nanostructures prepared by immersing the undoped PANI membranes (5 mm × 5 mm pieces) in a mixture solution of 0.1 M PVP and 5 mM $HAuCl_4$ for (A, B) 5, (C, D) 15, (E, F) 30, and (G, H) 60 min. The growth of Au nanostructures was carried out in an oven kept at 80 °C. Inset in E shows a high-resolution TEM image of a single Au nanoneedle.

The XRD patterns of these time correlated Au nanostructures show diffraction peaks that can be well indexed to the (111), (200), (220), (311), and (222) crystal planes of face-center-cubic (fcc) Au crystals (Figure 4). However, it is

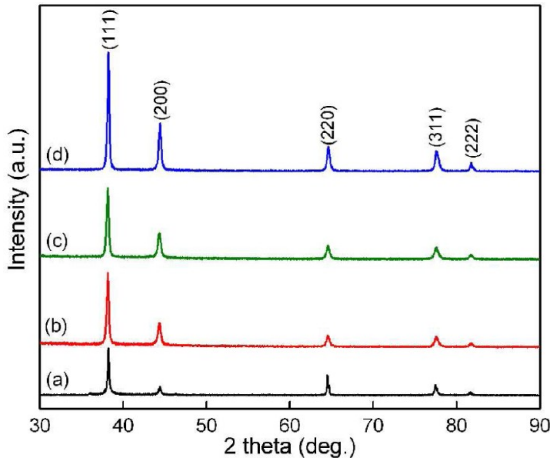

Figure 4. XRD patterns of Au nanostructures prepared by immersing the undoped PANI membrane in a mixture solution of 0.1 M PVP and 5 mM $HAuCl_4$ for (a) 5, (b) 15, (c) 30, and (d) 60 min.

calculated that the intensity ratio of (111) and (200) planes, $I(111)/I(200)$, decreases as the reaction time is increased, which is 6.55, 4.21, 3.16, and 2.49 for the Au nanostructures produced at 5, 15, 30, and 60 min, respectively, as compared to a number of about 1.90 for bulk Au crystals.[43,44] This trend indicates that at initial low reaction times, the needlelike Au nanostructures preferably grow along the (111) direction, which then ripen into more bulklike Au crystallites at long reaction times. The high-resolution TEM image in Figure 3E also confirms that these Au nanoneedles preferably grow along the (111) crystal plane.

We are especially interested in these thorny Au nanostructures as their nanoscale features are currently thought to be necessary for efficient SERS enhancement. Though PVP molecules will be inevitably present on the Au nanostructures even after repeated rinsing, PVP will not affect the SERS measurement as no Raman peaks due to PVP are detected. PVP may mainly adsorb onto areas away from the plasmon hot spots on the Au structures, which may actually improve SERS sensitivity because of passivation of Au surface that does not contribute to the SERS enhancement.[45] Concentration studies with 4-MBA using these thorny Au nanostructures show an increase of 3 orders of magnitude in the detection limit (1×10^{-9} M, sub-parts per billion level) relative to the featureless Au (Figure 5). These data were recorded from the Au nanostructures produced at a reaction time of 30 min (Figure 3E, F), which is comparable to the best sensitivities of Au substrates ever reported.[20,46] No Raman features of 4-MBA can be found with a concentration of 1×10^{-10} M or lower. Au nanostructures prepared at a reaction time of 5 and 15 min display similar SERS performances (see Figure S4 in the

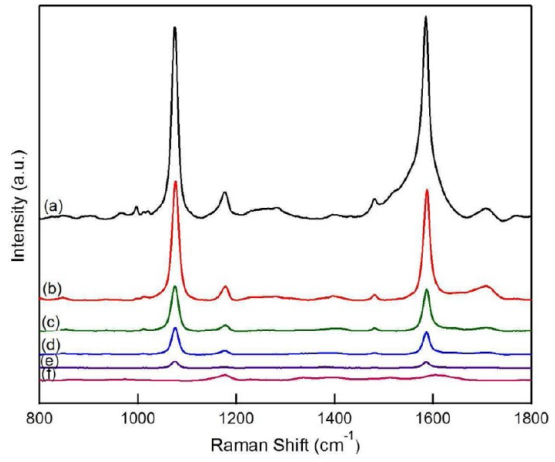

Figure 5. Concentration-dependent SERS spectra of 4-MBA on the Au nanostructures prepared by immersing the undoped PANI membrane in a mixture solution of 0.1 M PVP and 5 mM $HAuCl_4$ for 30 min (see Figures 3E, F): (a) 1×10^{-2} M, (b) 1×10^{-4} M, (c) 1×10^{-6} M, (d) 1×10^{-8} M, (e) 1×10^{-9} M, (f) 1×10^{-10} M.

dx.doi.org/10.1021/am301881q | ACS Appl. Mater. Interfaces 2013, 5, 49−54

Supporting Information). However, the Au nanostructures at a reaction time of 60 min can only detect 4-MBA at a concentration of 1×10^{-6} M or higher (see Figure S5 in the Supporting Information). It is believed that higher surface areas of the as-prepared thorny Au nanostructures and thus more target molecules adsorbed on the Au surfaces will contribute to the superior SERS behaviors. Meanwhile, the special geometric features can also lead to more SERS hot spots in those structures, as found in the assemblies of Au nanoparticles.[47−49] To demonstrate the generality of these Au nanostructures for SERS application, we also measured their SERS response toward another analyte, Rhodamine B, which shows that a similar sensitivity of 1×10^{-9} M can be reached (see Figure S6 in the Supporting Information).

4. CONCLUSIONS

In summary, we have demonstrated the fabrication of Au nanostructures on undoped PANI surfaces through spontaneous chemical reduction by conducting polymer for SERS applications. Acid doping of the growth solutions leads to homogeneous Au structures on the PANI substrates; however their limited surface area and lack of nanoscale morphology limit their overall SERS activity only at subppm level. Controlled Au growth from a reaction system consisting of 5 mM $HAuCl_4$ and 0.1 M PVP at 80 °C leads to thorny Au nanostructures, which allows a significant increase in SERS sensitivity and an ultimate detection limit up to 1×10^{-9} M (sub-ppb level) for two different analyte molecules, 4-mercaptobenzoic acid and Rhodamine B. We believe this facile synthetic approach to Au nanostructures may open up new avenues for highly sensitive SERS-active materials for the trace detection of chemical and biological molecules.

■ ASSOCIATED CONTENT

Supporting Information

SEM images, TEM image, and Raman spectra. This material is available free of charge via the Internet at http://pubs.acs.org.

■ AUTHOR INFORMATION

Corresponding Author

*E-mail: pxu@hit.edu.cn (P.X.); hwang@lanl.gov (H.L.W.).

Notes

The authors declare no competing financial interest.

■ ACKNOWLEDGMENTS

P.X. thanks the support from the China Postdoctor Fund, NSFC (21203045, 21101041, 21003029, 21071037, 91122002), Fundamental Research Funds for the Central Universities (Grants HIT. NSRIF. 2010065 and 2011017, and HIT.BRETIII. 201223), and Director's Postdoctoral Fellow from LANL. H.L.W. acknowledges the financial support from the Laboratory Directed Research and Development (LDRD) fund under the auspices of DOE, BES Office of Science, and the National Nanotechnology Enterprise Development Center (NNEDC). This work was performed in part at the U.S. Department of Energy, Center for Integrated Nanotechnologies, at Los Alamos National Laboratory (Contract DE−AC52−06NA25396) and Sandia National Laboratories (Contract DE−AC04−94AL85000).

■ REFERENCES

(1) Sharma, B.; Frontiera, R. R.; Henry, A. I.; Ringe, E.; Van Duyne, R. P. *Mater. Today* **2012**, *15*, 16.
(2) Dieringer, J. A.; Wustholz, K. L.; Masiello, D. J.; Camden, J. P.; Kleinman, S. L.; Schatz, G. C.; Van Duyne, R. P. *J. Am. Chem. Soc.* **2009**, *131*, 849.
(3) Lim, D. K.; Jeon, K. S.; Hwang, J. H.; Kim, H.; Kwon, S.; Suh, Y. D.; Nam, J. M. *Nat. Nanotechnol.* **2011**, *6*, 452.
(4) Kneipp, K.; Wang, Y.; Kneipp, H.; Perelman, L. T.; Itzkan, I.; Dasari, R.; Feld, M. S. *Phys. Rev. Lett.* **1997**, *78*, 1667.
(5) Nie, S. M.; Emery, S. R. *Science* **1997**, *275*, 1102.
(6) Kodiyath, R.; Wang, J.; Combs, Z. A.; Chang, S.; Gupta, M. K.; Anderson, K. D.; Brown, R. J. C.; Tsukruk, V. V. *Small* **2011**, *7*, 3452.
(7) Sun, M.; Xu, H. *Small* **2012**, *8*, 2777.
(8) Fleischm., M.; Hendra, P. J.; Mcquilla, A. *Chem. Phys. Lett.* **1974**, *26*, 163.
(9) Albrecht, M. G.; Creighton, J. A. *J. Am. Chem. Soc.* **1977**, *99*, 5215.
(10) Jeanmarie, D. L.; van Duyne, R. P. *J. Electroanal. Chem.* **1977**, *84*, 1.
(11) Freeman, R. G.; Grabar, K. C.; Allison, K. J.; Bright, R. M.; Davis, J. A.; Guthrie, A. P.; Hommer, M. B.; Jackson, M. A.; Smith, P. C.; Walter, D. G.; Natan, M. J. *Science* **1995**, *267*, 1629.
(12) Gupta, M. K.; Chang, S.; Singamaneni, S.; Drummy, L. F.; Gunawidjaja, R.; Naik, R. R.; Tsukruk, V. V. *Small* **2011**, *7*, 1192.
(13) Hulteen, J. C.; Treichel, D. A.; Smith, M. T.; Duval, M. L.; Jensen, T. R.; Van Duyne, R. P. *J. Phys. Chem. B* **1999**, *103*, 3854.
(14) Sun, Y. G.; Pelton, M. *J. Phys. Chem. C* **2009**, *113*, 6061.
(15) Chen, A. Q.; DePrince, A. E.; Demortiere, A.; Joshi-Imre, A.; Shevchenko, E. V.; Gray, S. K.; Welp, U.; Vlasko-Vlasov, V. K. *Small* **2011**, *7*, 2365.
(16) Rycenga, M.; Camargo, P. H. C.; Li, W. Y.; Moran, C. H.; Xia, Y. N. *J. Phys. Chem. Lett.* **2010**, *1*, 696.
(17) McLellan, J. M.; Li, Z. Y.; Siekkinen, A. R.; Xia, Y. N. *Nano Lett* **2007**, *7*, 1013.
(18) Zhu, Y. Y.; Kuang, H.; Xu, L. G.; Ma, W.; Peng, C. F.; Hua, Y. F.; Wang, L. B.; Xu, C. L. *J. Mater. Chem.* **2012**, *22*, 2387.
(19) He, L. F.; Huang, J. A.; Xu, T. T.; Chen, L. M.; Zhang, K.; Han, S. T.; He, Y.; Lee, S. T. *J. Mater. Chem.* **2012**, *22*, 1370.
(20) Kumari, G.; Narayana, C. *J. Phys. Chem. Lett.* **2012**, *3*, 1130.
(21) Sun, Y. G.; Wiederrecht, G. P. *Small* **2007**, *3*, 1964.
(22) Ko, H.; Singamaneni, S.; Tsukruk, V. V. *Small* **2008**, *4*, 1576.
(23) He, H.; Cai, W.; Lin, Y.; Chen, B. *Chem. Commun.* **2010**, *46*, 7223.
(24) Chan, S.; Kwon, S.; Koo, T. W.; Lee, L. P.; Berlin, A. A. *Adv. Mater.* **2003**, *15*, 1595.
(25) Chen, L. M.; Luo, L. B.; Chen, Z. H.; Zhang, M. L.; Zapien, J. A.; Lee, C. S.; Lee, S. T. *J. Phys. Chem. C* **2010**, *114*, 93.
(26) Sinha, G.; Depero, L. E.; Alessandri, I. *ACS Appl. Mater. Interfaces* **2011**, *3*, 2557.
(27) Musumeci, A.; Gosztola, D.; Schiller, T.; Dimitrijevic, N. M.; Mujica, V.; Martin, D.; Rajh, T. *J. Am. Chem. Soc.* **2009**, *131*, 6040.
(28) Wang, Y. F.; Ruan, W. D.; Zhang, J. H.; Yang, B.; Xu, W. Q.; Zhao, B.; Lombardi, J. R. *J. Raman Spectrosc.* **2009**, *40*, 1072.
(29) Xu, P.; Akhadov, E.; Wang, L. Y.; Wang, H. L. *Chem. Commun.* **2011**, *47*, 10764.
(30) Xu, P.; Jeon, S. H.; Chen, H. T.; Luo, H. M.; Zou, G. F.; Jia, Q. X.; Anghel, M.; Teuscher, C.; Williams, D. J.; Zhang, B.; Han, X. J.; Wang, H. L. *J. Phys. Chem. C* **2010**, *114*, 22147.
(31) Xu, P.; Jeon, S. H.; Mack, N. H.; Doorn, S. K.; Williams, D. J.; Han, X. J.; Wang, H. L. *Nanoscale* **2010**, *2*, 1436.
(32) Xu, P.; Mack, N. H.; Jeon, S. H.; Doorn, S. K.; Han, X. J.; Wang, H. L. *Langmuir* **2010**, *26*, 8882.
(33) Xu, P.; Zhang, B.; Mack, N. H.; Doorn, S. K.; Han, X. J.; Wang, H. L. *J. Mater. Chem.* **2010**, *20*, 7222.
(34) Zhang, B.; Xu, P.; Xie, X. M.; Wei, H.; Li, Z. P.; Mack, N. H.; Han, X. J.; Xu, H. X.; Wang, H. L. *J. Mater. Chem.* **2011**, *21*, 2495.
(35) Xu, P.; Han, X. J.; Wang, C.; Zhang, B.; Wang, X. H.; Wang, H. L. *Macromol. Rapid Commun.* **2008**, *29*, 1392.

(36) Yan, J.; Han, X. J.; He, J. J.; Kang, L. L.; Zhang, B.; Du, Y. C.; Zhao, H. T.; Dong, C. K.; Wang, H. L.; Xu, P. *ACS Appl. Mater. Interfaces* **2012**, *4*, 2752.
(37) Gao, Y.; Chen, C. A.; Gau, H. M.; Bailey, J. A.; Akhadov, E.; Williams, D.; Wang, H. L. *Chem. Mater.* **2008**, *20*, 2839.
(38) Shih, H. H.; Williams, D.; Mack, N. H.; Wang, H. L. *Macromolecules* **2009**, *42*, 14.
(39) Michota, A.; Bukowska, J. *J. Raman Spectrosc.* **2003**, *34*, 21.
(40) Sun, Y. G.; Mayers, B.; Herricks, T.; Xia, Y. N. *Nano Lett.* **2003**, *3*, 955.
(41) Xiong, Y. J.; Chen, J. Y.; Wiley, B.; Xia, Y. N.; Yin, Y. D.; Li, Z. Y. *Nano Lett.* **2005**, *5*, 1237.
(42) Sun, Y. G.; Yin, Y. D.; Mayers, B. T.; Herricks, T.; Xia, Y. N. *Chem. Mater.* **2002**, *14*, 4736.
(43) Manoj, R.; Dipanwita, M.; Md. Harunar, R.; Mandal, T. K. *J. Mater. Chem.* **2012**, *22*, 18335.
(44) Kim, F.; Connor, S.; Song, H.; Kuykendall, T.; Yang, P. D. *Angew. Chem., Int. Ed.* **2004**, *43*, 3673.
(45) Zhao, Y.; Newton, J. N.; Liu, J.; Wei, A. *Langmuir* **2009**, *25*, 13833.
(46) Hsieh, H. Y.; Xiao, J. L.; Lee, C. H.; Huang, T. W.; Yang, C. S.; Wang, P. C.; Tseng, F. G. *J. Phys. Chem. C* **2011**, *115*, 16258.
(47) Zhang, C. L.; Lv, K. P.; Cong, H. P.; Yu, S. H. *Small* **2012**, *8*, 648.
(48) Zhu, Z. N.; Meng, H. F.; Liu, W. J.; Liu, X. F.; Gong, J. X.; Qiu, X. H.; Jiang, L.; Wang, D.; Tang, Z. Y. *Angew. Chem., Int. Ed.* **2011**, *50*, 1593.
(49) Taylor, R. W.; Lee, T. C.; Scherman, O. A.; Esteban, R.; Aizpurua, J.; Huang, F. M.; Baumberg, J. J.; Mahajan, S. *ACS Nano* **2011**, *5*, 3878.